Percolation Threshold and Depression in Properties of Polymer Nanocomposites

Ricardo Ritter de Souza Barnasky[a]* [ID], *Juliana Cristina Frankowiak[a]* [ID], *Carlos Vinícios Opelt[b]* [ID],

Luiz Antonio Ferreira Coelho[a] [ID]

[a]*Universidade do Estado de Santa Catarina, Centro de Ciências Tecnológicas (CCT), Joinville, SC, Brasil.*
[b]*Centro Universitário Católico de Santa Catarina, Joinville, SC, Brasil.*

Percolation threshold is an important phenomenon to be addressed when producing nanocomposites, especially because the literature suggests a depression of properties near this region. In this study, epoxy matrix nanocomposites were produced with different volume fractions of multi-walled carbon nanotubes and were characterized according to their electrical, thermal, and mechanical properties. In addition, digital image correlation (DIC) was used to measure the strain of nanocomposites and to show how it behaves in different percolation states. Electrical conductivity indicated a percolation threshold near 0.22% v/v of nanoparticles. Differential scanning calorimetry analysis showed a depression followed by an increase in glass transition temperature near the percolation threshold. Tensile strength tests presented a depression followed by an increasing near percolation threshold. DIC images showed that nanocomposites present a different behavior when near the percolation threshold, with a more distributed strain over the surface of the sample under stress and fracture toughness decreased near the percolation threshold.

Keywords: *Percolation Threshold, Carbon nanotubes, Interphase, Nanocomposites.*

1. Introduction

An important aspect of nanocomposites is the elevated surface area of the nanomaterial per volume unit when compared to microcomposites. This characteristic influences directly on interphase phenomena and, consequently, the final properties of these nanocomposites[1].

One may define the interphase as a zone of transition between the nanoparticle interface and the polymer bulk, which can lead to a change of morphological, chemical, mechanical, and physical properties of the final material, differing from the bulk or the isolated nanoparticle, which, may appear as an unexpected or unwanted characteristic in nanocomposites[2-5].

Therefore, nanocomposites present a considerable volume of interphase, and variations of properties can be observed with few percentages of nanoparticles when compared to their pure polymer matrix[6]. When these regions of interphase connect throughout the whole material occurs the percolation of interphase, which may lead to a different behavior[7]. Thus, nanocomposites may present distinct properties before, after, or near the percolation threshold[8]. Hence, the percolation threshold influences directly the final properties of nanocomposites[4,5,9].

The knowledge of the percolation threshold is also important because it may be used as a point of optimization of properties, for example, controlling the dispersed phase and decreasing the percolation threshold[10] to achieve conductive nanocomposites with an ultra-low percolation threshold[11,12], or to predict the approximation of discrete parts of interphases[7], or even to simulate and measure the percolation in experimental studies[13,14].

Despite the different changes in the material during the occurrence and increase of the percolation state, electrical conductivity is one of the most characteristic properties that can be observed and measured when adding conductive nanoparticles to a dielectric matrix. This happens because the incorporation of conductive nanoparticles increases the probabilities of conductive path formation[15] until it reaches a critical value and the nanocomposite changes from dielectric to dissipative or conductive, which is also indicated as the percolation threshold[16-24]. Moreover, the state of percolation in nanocomposites also presents changes on mechanical properties, which can be enhanced with low volume fractions of nanoparticles[25] or present discontinuities, caused by local perturbations on polymer chains, leading to a degradation mechanism of mechanical properties[8].

The percolation state of nanocomposites may be verified by using different techniques, with electrical percolation the most established technique when considering the addition of conductive nanoparticles in a dielectric matrix.

As the percolation threshold may act directly on other material properties, the glass transition temperature (Tg) of materials may also change, exhibiting both an increase or

*e-mail: ricardo.barnasky@gmail.com

a decrease in Tg, which is related to interactions between polymer chains with the surface of nanoparticles[26-30].

Digital image correlation (DIC) is an ongoing technique for materials characterization, which uses optical and numerical data to determine the displacement on the surface of samples under mechanical loading and compare this changing of position, providing a more accurate technique for measuring strain[31-33]. Although there is still a lack of comprehensive studies in the area showing that DIC can also be used to locate surface deformations of nanocomposites and their relation with a percolated network on their structure. Thus, this study aims to evaluate the electrical, thermal, and mechanical properties of nanocomposites in stages below, above, and near the percolation threshold, as well as it is employed the use of digital image correlation technique as a tool to visualize how strain is distributed over the nanocomposites in these three main stages.

2. Experimental

2.1. Materials

The polymeric matrix was a low viscosity epoxy resin SQ2004F monomer (500 cPs, 20ºC) and a SQ3154 hardener (<200 cPs, 20ºC) produced by Silaex Química Ltd, with density of 1.09 g.cm^{-3}. The nanoparticles were multi-walled carbon nanotubes (MWCNTs) TNIM4, produced by Chengdu Organic Chemicals Co. Ltd, with outer diameter between 10 nm and 30 nm, length between 10 µm and 30 µm, surface area of 140 m^2.g^{-1} and density of 2.1 g. cm^{-3}.

2.2. Methods

Nanocomposites were produced using different quantities of nanoparticles as presented in Table 1. The monomer/hardener ratio was the same of 100:50 for all samples, as indicated by the supplier, and the amounts of CNTs were chosen based on previous work[34-37] and the maximum capacity of CNTs addition in epoxy matrix.

The nanocomposites processing followed the steps presented in Figure 1. Initially, nanoparticle amounts were added to the monomer and mixed for 20 minutes in a magnetic stirrer to a previous homogenization and kept under stirring to the application of a high energy sonication process using a Sonics VCX750, in a constant amount of 400 J/g. After sonication, the solution was kept under stirring until reached room temperature. Then, the hardener was added to the mixture and kept under stirring for more 20 minutes. The mixtures were poured into molds according to the dimensions of test specimens of ASTM D638 (Type IV) and

ASTM D5045 standards and the curing process was done at room temperature for 7 days, as indicated by the epoxy resin supplier. The production of samples without nanoparticles was conducted directly in the step of hardener addition and stirring for 20 minutes.

2.3. Characterization

2.3.1. Electrical characterization

Electrical conductivity was measured according to electrical impedance spectroscopy[35-37] in an Agilent – Precision Impedance Analyzer 4294, measuring 500 points between 40 Hz and 40 MHz, in 5mV AC, at room temperature.

2.3.2. Thermal characterization

Differential scanning calorimetry (DSC) was applied to verify the glass transition of samples, using a NETZSCH STA 449 F3 Jupiter®, in a N$_2$ atmosphere with a first heating cycle (for stress-relief purposes) of 10ºC/min and a second heating cycle of 10ºC/min, from 30ºC to 250ºC. Glass transition temperature was determined in second heating, at the inflection point, using the equipment proper software, NETZSCH Proteus.

2.3.3. Mechanical characterization

Tensile strength tests were conducted in five samples according to ASTM D638 properties of five samples were determined according to ASTM D638 standard, conducted in an AME 5kN – Filizola machine, with a load cell of 5kN, test speed of 5 mm/min, and data acquisition rate of 300 points per minute (5Hz). In these tests, yield strength values of samples were measured considering the first point at which an increase in strain occurs without an increase in stress, and ultimate tensile strength was considered as the value of stress at break.

Fracture toughness (K_{ic}) tests were conducted according to ASTM D5045, in five samples with a compact tension (CT) shape, speed test of 10 mm/min, and data acquisition of 5 Hz in an opening mode I.

2.3.4. Digital image correlation

Specimens were prepared in two steps: first, samples were painted with a thin layer of matte white spray paint

Table 1. Description of groups.

Group	Φ vol. (%)
000	0.00
015	0.15
022	0.22
050	0.50
150	1.50
220	2.20

Note: Φ vol. = volume fraction.
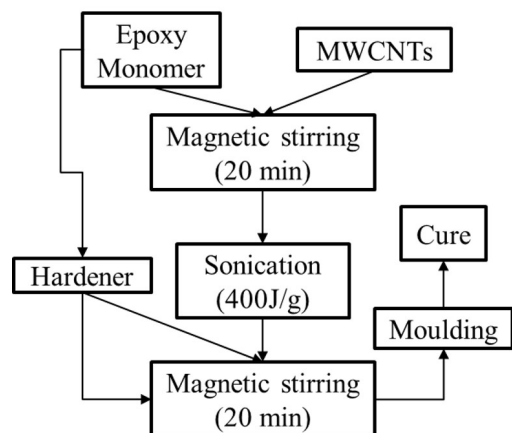
Figure 1. Flow diagram of the experimental procedure.

(Figure 2a), and then matte black spray paint was pulverized over white paint (Figure 2b) to allow contrast calibration of the equipment. The digital image correlation (DIC) technique was applied using a Dantec Dynamics Q-400, with two 4MPix cameras adjusted as shown in Figure 3, and with a frame acquisition rate of 5Hz to allow the pairing between DIC and mechanical stress data.
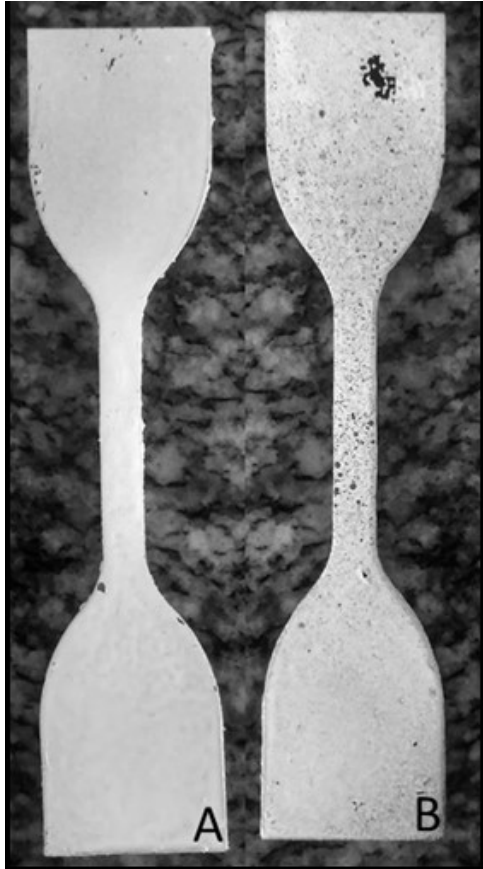
Figure 2. Sample preparation in A, painted with a thin layer of matte white spray paint and in B, after the pulverization with matte black spray paint.

3. Results and Discussion

3.1. Impedance spectroscopy

Results of electrical conductivity are shown in Figure 4 and Figure 5. Figure 4 shows electrical conductivity as a function of frequency, for each group of nanocomposites. In all samples, it is verified an increase in conductivity as the frequency increases. Similar behavior was reported in the literature and it is attributed to dipole and interface polarization processes. In this behavior, charges move from one place to another inside the dielectric material in frequencies up to 10^3 Hz (interfacial polarization), and charges locally bonded to atoms and molecules move in frequencies up to 10^7 Hz (dipolar polarization)[38].

As Figure 4 also shows an overlap of initial curves, Figure 5 presents data of electrical conductivity as a function of nanoparticles fraction, in which is possible to verify that there is a jump in conductivity after 0.15% v/v up to 0,50% v/v, where electrical conductivity stabilizes in a linear increasing, indicating an already percolated state. Thus, it was established the sample in 0.22% as the closest one near the percolation threshold, indicated by the gray area in Figure 5. It should be noted that even the electrical conductivity presented a depression in the gray region followed by an increase. Very probably a trap for charges at interphases overlap is created near the percolation threshold as already pointed out in the literature[5].

3.2. Glass transition temperature

Results of the DSC analysis are presented in Figure 6 and Figure 7, which showed a change of behavior in glass transition temperature for sample in percolation threshold. While Figure 6 presents DSC traces of second heating, Figure 7 summarizes the results of the inflection point, as indicated by equipment software. The epoxy matrix, as detailed in Figure 7, presents a Tg of 71°. There is a decrease in Tg for 0.15% v/v, where Tg is 68°C followed by an increase in Tg for 76°C for sample 0.22% v/v in percolation threshold, followed by a decrease in Tg for all samples above the percolation threshold.

It was noted that a percolated interphase network has a significant effect on Tg, by acting on the properties.
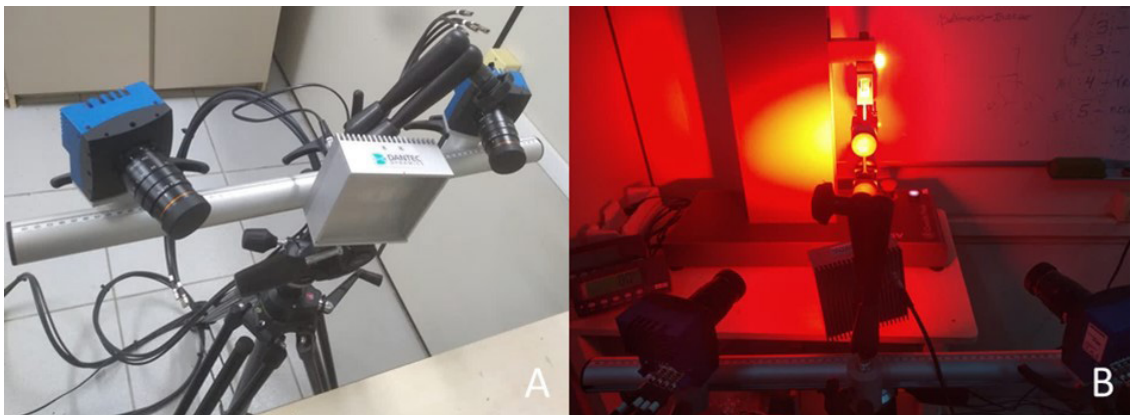
Figure 3. Apparatus of DIC.
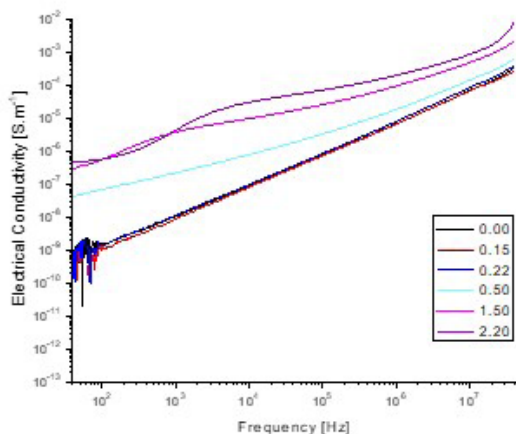
Figure 4. Electrical conductivity of nanocomposites according to frequency.
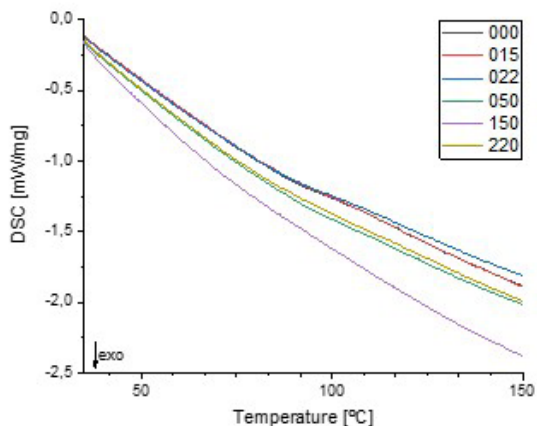
Figure 6. DSC traces of samples.
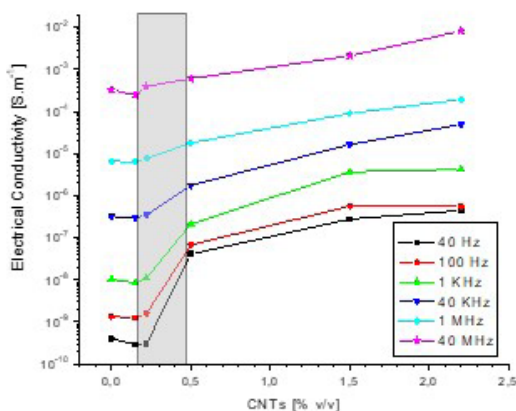
Figure 5. Electrical conductivity of nanocomposites according to nanotubes fractions in different frequencies. The percolation threshold is indicated by the gray area.
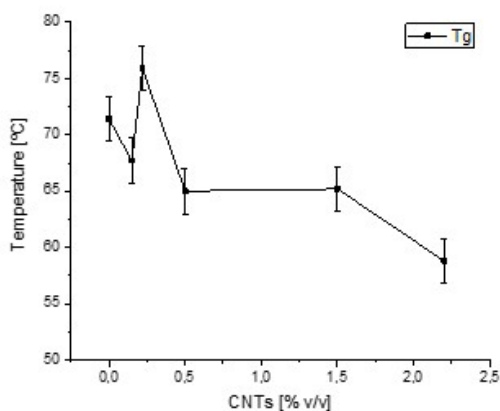
Figure 7. Glass transition temperature of samples.

As nanoparticles may produce agglomeration clusters, it was reported that these clusters lead to a decrease of interphase, not only because the interphase in agglomerated clusters overlaps, but also because a disappearance of the interphase network in the matrix may happen and it may produce effects on properties according to its stage of percolation. Below the percolation threshold, the effect of these clusters did not produce a pronounced change in Tg. Near the percolation threshold, as the paths are being formed, Tg changes significantly while after percolation, as the paths are saturated, Tg improvements decay above the percolation threshold.

An important fact of interphase on increasing Tg is the attractive interaction between nanofillers and polymer chains, which restricts the local mobility of these chains and significantly increases Tg[2,5,9,27].

At interphase polymer chains can have steric confinement, reducing their mobility and dipoles mobility[5], modifying crystallinity and chain network[12,39,40]. Concerning the effects of interphase on the Tg, it is important to highlight that there are opposing mechanisms acting, which make the

influence on the glass transition temperature not so clear. While the inclusion of rigid nanoparticles may restrain the movements of polymer chains, (increasing Tg), it may also locally disrupt cross-link, which ends up in a slight decrease in the Tg. The last one is particularly important in case there no effective functionalization techniques are employed[41].

Another important aspect to be considered is that interphases have at least two layers, also called double layer interphase model, which present one tightly bonded layer to the nanoparticle and the other is weaker connected. The double layer interphase model also presents a reliable model to explain a gradient of properties toward the matrix material[42]. Hence, it is suggested that when the inner layer is bonded to the nanoparticle, it leads to a formation of a glassy chain, formed by a dynamically frozen polymer layer[43,44].

3.3. Mechanical properties and digital image correlation

The typical behavior of each group of nanocomposites under the tensile strength test is presented in Figure 8, represented by average curves of samples and their numerical
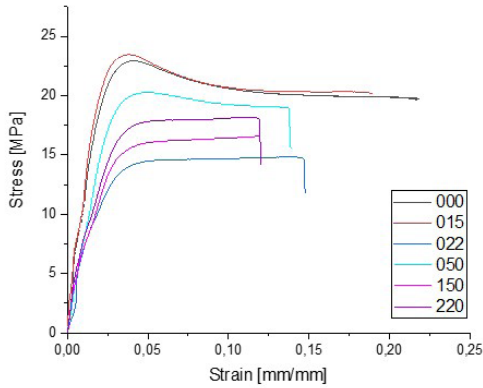
Figure 8. Representative curves of tensile strength tests.

Figure 9. Digital images for tensile tested nanocomposites.

results are presented in Table 2, as well as analysis of variance (ANOVA) and Tukey's test at 5% of representative level.

It is important to highlight that the obtained data for the epoxy matrix is in accordance with the supplier and also the available literature[45]. In comparison to electrical conductivity, it is possible to verify an increase in mechanical properties with the addition of 0.15% v/v of MWCNTs. However, there is a decrease in mechanical properties above this value, reaching the minimum value for the sample with 0.22% v/v in the percolation threshold.

Images taken using DIC cameras were normalized in a range between 0% and 5% of strain, represented by colors from deep blue to red, and greyish red for points above this range. Figure 9 shows the frames taken when samples reached yield strength.

It is possible to visualize in Figure 9 that samples present distinct behaviors according to the percentage of MWCNTs. The epoxy matrix showed typical behavior of tensile test, with the strain concentrated in a narrow region section, as represented by the grayish points. As impedance spectroscopy showed an increase in electrical conductivity after 0.22%, v/v and there is the percolation threshold near this point, the nanocomposite with 0.22% v/v MWCNTs presents a highlighted behavior, in which the main portion of the specimen has grayish areas, showing that the strain is much more distributed along the sample. Although, it should be stressed that the tensile tests indicated that adhesion between matrix and nanoparticles at 0.22% v/v is very weak since the numerical value is the smallest of the studied samples. The ultimate tensile strength data indicated the adhesion is recovered at 0.50% v/v and after this composition is decreasing again.

On the other hand, samples above the percolation threshold recover their behavior of concentrating strain in specific regions and not over the whole surface. In order to evidence this strain distribution, Figure 10 shows images for samples without, near, and after the percolation threshold. As Figure 10 demonstrates this behavior, Figure 11 shows the connection between the images and the tested results of yield strength in tensile tests.

As seen in previous works of our research group[35,46-48], failure mechanisms such as crack bridging – pull-out, crack
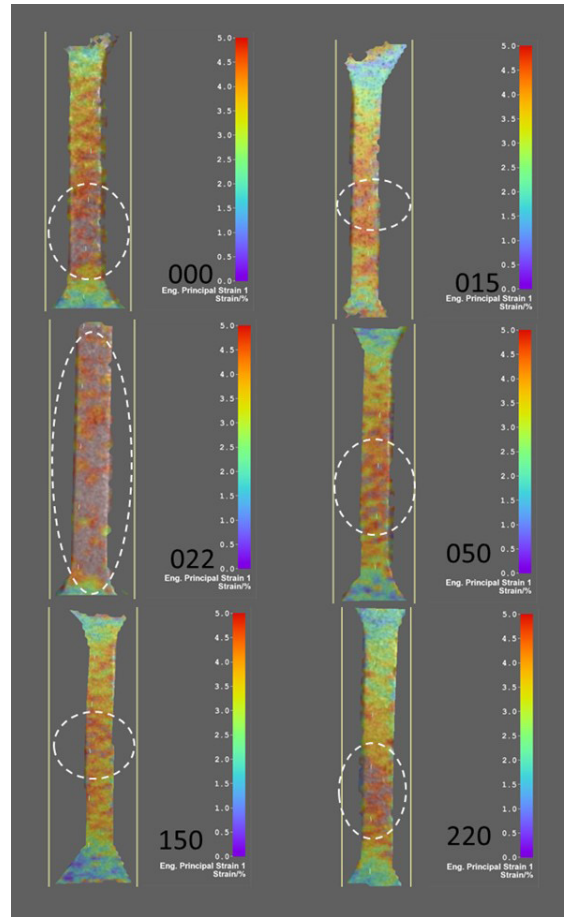
Table 2. Analysis of variance and Tukey's test at 5% of significance level of tensile strength tests.

Group	Yield Strength [MPa]	Ultimate Tensile Strength [MPa]
000	22.94 (1.86) a	22.94 (1.86) a
015	23.47 (2.88) a	23.47 (2.88) a
022	14.38 (1.41) c	16.78 (1.02) c
050	20.43 (1.09) ab	20.92 (1.22) ab
150	15.78 (2.40) c	17.45 (2.41) bc
220	17.76 (1.88) bc	18.97 (1.82) bc

Note: Standard deviation values are in parenthesis. Means followed by the same letter do not significantly differ, by Tukey's test at 5% of significance level.

deflection, and crack pinning tend to occur in the interphase. This is especially true when strong nanoparticle-matrix interactions promote the formation of brittle interphase, through which the crack propagates. In these cases, the percolation threshold may lead to less energy dissipation during crack growth, since these interphases may act as a region of weakness for mechanical properties[49]. As the percolation threshold in nanocomposites indicates the minimum concentration of a nanomaterial necessary to form a kind of continuous path network[50], this amount may not
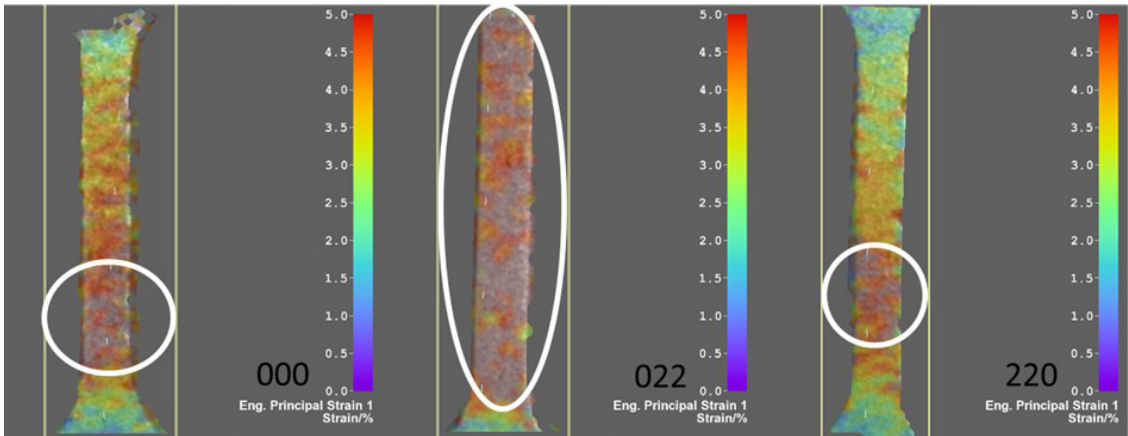
Figure 10. Strain distribution over sample surface in the polymer matrix (000), near percolation threshold (022), and after percolation (220).
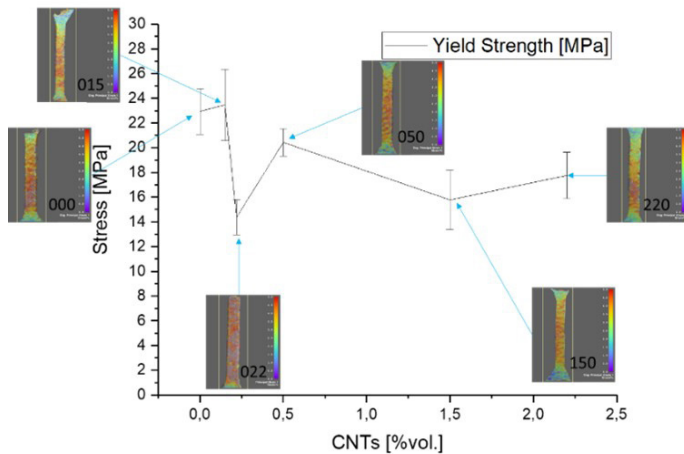
Figure 11. Digital images of nanocomposite samples and their values of yield strength in a tensile strength test.

be enough to guarantee that reinforcement occurs. Instead, stress and strain have this weak region be distributed, as yield strength presents a drop in value, due to a reduction of constraints on the polymer network[51].

The obtained results of mechanical strength, its relation with electrical percolation, and the behavior observed from DIC images are in agreement between them and in accordance with simulation methods[51], which also predict a yield drop and plastic weakening polymer nanocomposites near percolation, followed by a recovery of behavior after percolation.

The fracture toughness of samples is presented in Table 3, where it is also possible to verify a similar behavior of discontinuity of properties near the percolation threshold.

An important aspect observed is the relatively high fracture toughness of polymer matrix, when compared to other studies using epoxy resins[47,52-54] However, it is consistent with behavior presented in tensile strength tests, demonstrating that the chosen commercial resin has a considerable strain.

The increase in K_{ic} values is an expected behavior for percolated nanocomposites[55,56], although a decrease in K_{ic} was observed for the sample at the percolation threshold,

Table 3. Analysis of variance and Tukey's test at 5% of significance level of fracture toughness tests.

Group	K_{ic} [MPa.m$^{1/2}$]
000	2.59 (0.25) ab
015	2.86 (0.12) ab
022	2.49 (0.04) b
050	2.91 (0.12) ab
150	2.98 (0.18) a
220	2.52 (0.19) ab

Note: Standard deviation values are in parenthesis. Means followed by the same letter do not significantly differ, by Tukey's test at 5% of significance level.

as indicated in Table 3 and verified by tukey's test at 5% of significance level.

In terms of digital image correlation, Figure 12 shows the strain distribution over the surface of samples on fracture toughness tests taken in the last frame before crack propagating. It is detailed that the sample with 0.22%v/v, at the percolation threshold, presents a strain more distributed
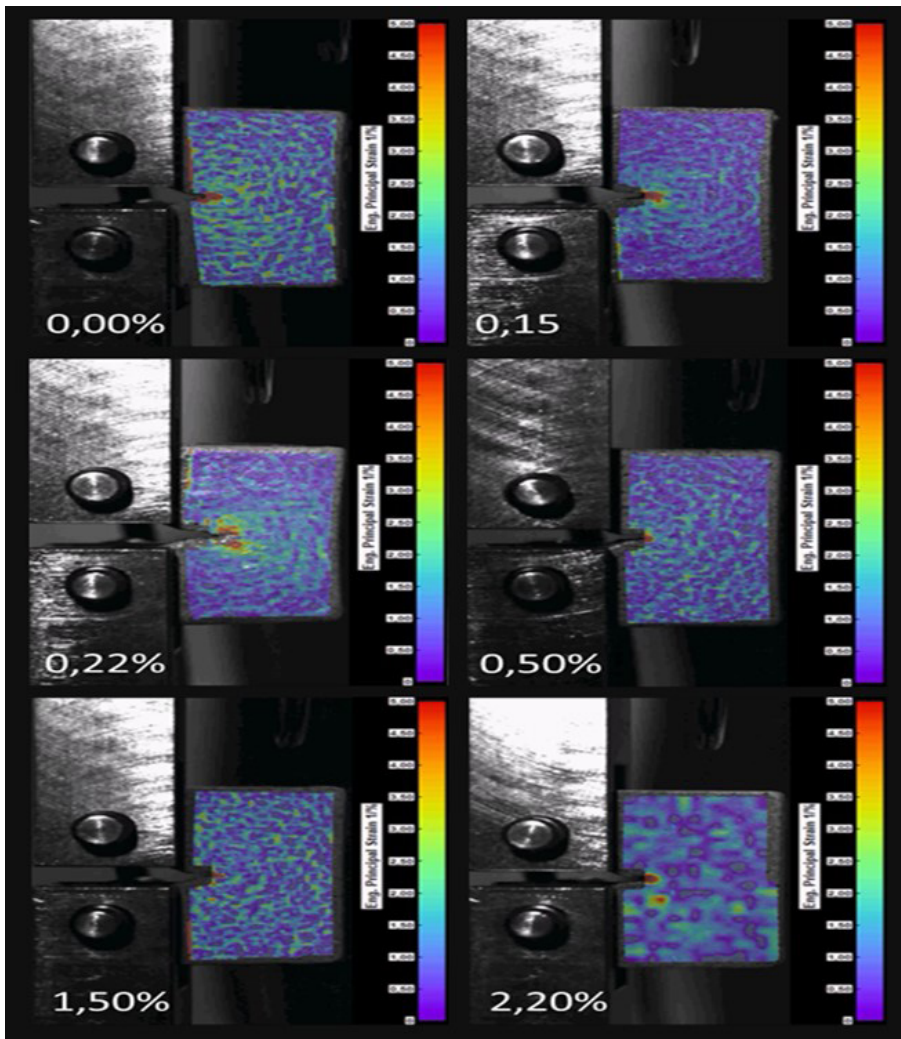
Figure 12. Digital images of fracture toughness tests.

over the surface, which is evidenced not only by the larger red area near the crack opening, but also by the yellow and green areas around the crack tip.

Another important aspect that corroborates this behavior, is that it is reported that carbon nanotubes may also present a weak interfacial bonding, which brings to lower fracture toughness of the specimens, acting as imperfection and reducing mechanical properties[56,57].

4. Conclusions

Epoxy matrix nanocomposites were produced with different percentages of MWCNTs and were characterized according to their electrical, thermal, and mechanical properties.

Impedance spectroscopy showed a decrease in the electrical conduction at very low fractions of MWCNTs, an increase in samples after 0.22% v/v of MWCNTs, with a relevant increase on samples with 0.50% v/v of MWCNTs, indicating the range after 0.15% v/v and 0.50% v/v as the lower and upper limits of percolation, and sample with 0.22% v/v as the sample in this threshold.

An interesting behavior of glass transition temperature right on the percolation threshold was detected, with an increase of this temperature for the sample with 0.22% v/v of MWCNTs, followed by a decrease of Tg on samples already percolated. This behavior is attributed to a critical amount of interphase which has bounded polymer chains, forming a glassy layer, with strong interaction between the polymer layer and nanoparticles.

Mechanical characterization also showed a change in mechanical properties near the percolation threshold. The behavior of strain under tensile tests was evidenced by the digital image correlation technique, which also revealed that samples near percolation present a different mechanical behavior than samples before or after this threshold.

Considering the existence of the glassy, strong bounded polymer layer around nanoparticles, the percolation path may also form a glassy and thin layer, which acts like a polymer shell, with fragile behavior. As the inner layer around nanoparticles also acts as a stress distributor, this may explain how strain is distributed over the surface of the sample near the percolation threshold.

Regarding this glassy shell around nanoparticles, it would both explain the decreasing of mechanical properties, with the lower tensile strength at percolation and the behavior observed on fracture toughness tests, which also presented a decrease of K_{ic}. Moreover, although the interphase of nanoparticles and polymer matrix may present a strong interaction, the interfacial bonding between this interphase and the whole matrix is weak bonded, leading to the behavior observed in this study.

5. Acknowledgments

6. References

1. Shaji A, Zachariah AK. Surface area analysis of nanomaterials. In: Thomas S, Thomas R, Zachariah AK, Mishra RK, editors. Thermal and rheological measurement techniques for nanomaterials characterization. Amsterdam: Elsevier; 2017. p. 197-231. http://dx.doi.org/10.1016/B978-0-323-46139-9.00009-8.

2. Wagner HD, Vaia RA. Nanocomposites: issues at the interface. Mater Today. 2004;7(11):38-42. http://dx.doi.org/10.1016/S1369-7021(04)00507-3.

3. Gao SL, Mäder E. Multifunctional interphases in polymer composites. In: Friedrich K, Breuer U, editors. Multifunctional polymer composites. Amsterdam: Elsevier; 2015. p. 338-62. http://dx.doi.org/10.1016/B978-0-323-26434-1.00010-6

4. Zare Y. An approach to study the roles of percolation threshold and interphase in tensile modulus of polymer/clay nanocomposites. J Colloid Interface Sci. 2017;486:249-54. http://dx.doi.org/10.1016/j.jcis.2016.09.080.

5. Karasinski EN, Sasse FD, Coelho LAF. Multifractal analysis of particle dispersion and interphase percolation in nanocomposites. Mater Res. 2018;21(5):e20180265. http://dx.doi.org/10.1590/1980-5373-mr-2018-0265.

6. Raetzke S, Kindersberger J. Role of interphase on the resistance to high-voltage arcing, on tracking and erosion of silicone/SiO$_2$ nanocomposites. IEEE Trans Electr Insul. 2010;17(2):607-14. http://dx.doi.org/10.1109/TDEI.2010.5448118.

7. Qiao R, Brinson LC. Simulation of interphase percolation and gradients in polymer nanocomposites. Compos Sci Technol. 2009;69(3-4):491-9. http://dx.doi.org/10.1016/j.compscitech.2008.11.022.

8. Shin H, Yang S, Choi J, Chang S, Cho M. Effect of interphase percolation on mechanical behavior of nanoparticle-reinforced polymer nanocomposite with filler agglomeration: a multiscale approach. Chem Phys Lett. 2015;635:80-5. http://dx.doi.org/10.1016/j.cplett.2015.06.054.

9. Li H, Zare Y, Rhee KY. The percolation threshold for tensile strength of polymer/CNT nanocomposites assuming filler network and interphase regions. Mater Chem Phys. 2018;207:76-83. http://dx.doi.org/10.1016/j.matchemphys.2017.12.053.

10. Ding Y, Zhou Q, Li X, Xiong Y, Guo S. PC light-scattering material containing "pomegranate-like" SAN-SiO2 microspheres with excellent effective scattering range based the large-screen display. Compos Sci Technol. 2021;201:108532. http://dx.doi.org/10.1016/j.compscitech.2020.108532.

11. Tu Z, Wang J, Yu C, Xiao H, Jiang T, Yang Y, et al. A Facile approach of preparation of polystyrene/graphene nanocomposites with ultra-low percolation threshold through an electrostatic assembly process. Compos Sci Technol. 2016;134:49-56. http://dx.doi.org/10.1016/j.compscitech.2016.08.003.

12. Du H, Spratford S, Shan JW, Weng GJ. Experimental and theoretical study of the evolution of fluid-suspended graphene morphology driven by an applied electric field and the attainment of ultra-low percolation threshold in graphene-polymer nanocomposites. Compos Sci Technol. 2020;199:108315. http://dx.doi.org/10.1016/j.compscitech.2020.108315.

13. Lu X, Zhang A, Dubrunfaut O, He D, Pichon L, Bai J. Numerical modeling and experimental characterization of the AC conductivity and dielectric properties of CNT/polymer nanocomposites. Compos Sci Technol. 2020;194:108150. http://dx.doi.org/10.1016/j.compscitech.2020.108150.

14. Jurča M, Vilčáková J, Gořalík M, Masař M, Ponížil P, Kazantseva N, et al. Reduced percolation threshold of conductive adhesive through nonuniform filler localization: monte Carlo simulation and experimental study. Compos Sci Technol. 2021;214:108964. http://dx.doi.org/10.1016/j.compscitech.2021.108964.

15. Gao Y, Ma R, Zhang H, Liu J, Zhao X, Zhang L. Controlling the electrical conductive network formation in nanorod filled polymer nanocomposites by tuning nanorod stiffness. RSC Advances. 2018;8(53):30248-56. http://dx.doi.org/10.1039/C8RA06264A.

16. Sandler JKW, Kirk JE, Kinloch IA, Shaffer MSP, Windle AH. Ultra-low electrical percolation threshold in carbon-nanotube-epoxy composites. Polymer. 2003;44(19):5893-9. http://dx.doi.org/10.1016/S0032-3861(03)00539-1.

17. Gelves GA, Lin B, Sundararaj U, Haber JA. Low electrical percolation threshold of silver and copper nanowires in polystyrene composites. Adv Funct Mater. 2006;16(18):2423-30. http://dx.doi.org/10.1002/adfm.200600336.

18. Bauhofer W, Kovacs JZ. A review and analysis of electrical percolation in carbon nanotube polymer composites. Compos Sci Technol. 2009;69(10):1486-98. http://dx.doi.org/10.1016/j.compscitech.2008.06.018.

19. Logakis E, Pissis P, Pospiech D, Korwitz A, Krause B, Reuter U, et al. Low electrical percolation threshold in poly(ethylene terephthalate)/multi-walled carbon nanotube nanocomposites. Eur Polym J. 2010;46(5):928-36. http://dx.doi.org/10.1016/j.eurpolymj.2010.01.023.

20. Zheng C, Zhao K, Shen H, Zhao X, Yao Z. Crack behavior in ultrafast laser drilling of thermal barrier coated nickel superalloy. J Mater Process Technol. 2020;282:116678. http://dx.doi.org/10.1016/j.jmatprotec.2020.116678.

21. Penu C, Hu G-H, Fernandez A, Marchal P, Choplin L. Rheological and electrical percolation thresholds of carbon nanotube/polymer nanocomposites. Polym Eng Sci. 2012;52(10):2173-81. http://dx.doi.org/10.1002/pen.23162.

22. Evgin T, Turgut A, Hamaoui G, Spitalsky Z, Horny N, Micusik M, et al. Size effects of graphene nanoplatelets on the properties of high-density polyethylene nanocomposites: morphological, thermal, electrical, and mechanical characterization. Beilstein J Nanotechnol. 2020;11:167-79. http://dx.doi.org/10.3762/bjnano.11.14.

23. Meisak D, Macutkevic J, Selskis A, Banys J, Kuzhir P. Dielectric properties and electrical percolation in MnFe$_2$O$_4$/epoxy resin composites. Phys Status Solidi. 2020;217(6):1900526. http://dx.doi.org/10.1002/pssa.201900526.

24. Alves AM, Cavalcanti SN, Silva MP, Freitas DMG, Agrawal P, Mélo TJA. Electrical, rheological, and mechanical properties copolymer/carbon black composites. J Vinyl Add Tech. 2021;27(2):445-58. http://dx.doi.org/10.1002/vnl.21818.

25. Baxter SC, Burrows BJ, Fralick BS. Mechanical percolation in nanocomposites: microstructure and micromechanics.

Probab Eng Mech. 2016;44:35-42. http://dx.doi.org/10.1016/j.probengmech.2015.09.018.

26. Su F, Miao M. Effect of MWCNT dimension on the electrical percolation and mechanical properties of poly(vinylidenefluoride-hexafluoropropylene) based nanocomposites. Synth Met. 2014;191:99-103. http://dx.doi.org/10.1016/j.synthmet.2014.02.023.

27. Ash BJ, Schadler LS, Siegel W. Glass transition behaviour of alumina/polymethylmethacrylate nanocomposites. Mater Lett. 2002;55(1-2):83-7. http://dx.doi.org/10.1016/S0167-577X(01)00626-7.

28. Wang SF, Ogale AA. Continuum space simulation and experimental characterization of electrical percolation behaviour of particulate composites. Compos Sci Technol. 1993;46(2):93-103. http://dx.doi.org/10.1016/0266-3538(93)90165-D.

29. Li C, Thostenson ET, Chou T-W. Effect of nanotube waviness on the electrical conductivity of carbon nanotube-based composites. Compos Sci Technol. 2008;68(6):1445-52. http://dx.doi.org/10.1016/j.compscitech.2007.10.056.

30. Rashmi P, Rajan JS. Effective use of nano-carbons in controlling the electrical conductivity of epoxy composites. Compos Sci Technol. 2021;202:108554. http://dx.doi.org/10.1016/j.compscitech.2020.108554.

31. Lecompte D, Vantomme J, Sol H. Crack detection in a concrete beam using two different camera techniques. Struct Health Monit. 2006;5(1):59-68. http://dx.doi.org/10.1177/1475921706057982.

32. Palanivelu S, De Pauw S, van Paepegem W, Degrieck J, van Ackeren J, Kakogiannis D, et al. Validation of digital image correlation technique for impact loading applications. In: DYMAT 2009 - 9th International Conference on the Mechanical and Physical Behaviour of Materials Under Dynamic Loading; 2009 Sep 7-11; Les Ulis, France. Proceedings. Madrid: DYMAT; 2009. p. 373-9. http://dx.doi.org/10.1051/dymat/2009053.

33. Omondi B, Aggelis DG, Sol H, Sitters C. Improved crack monitoring in structural concrete by combined acoustic emission and digital image correlation techniques. Struct Health Monit. 2016;15(3):359-78. http://dx.doi.org/10.1177/1475921716636806.

34. Haesch A, Clarkson T, Ivens J, Lomov SV, Verpoest I, Gorbatikh L. Localization of carbon nanotubes in resin rich zones of a woven composite linked to the dispersion state. Nanocomposites. 2015;1(4):204-13. http://dx.doi.org/10.1080/20550324.2015.1117306.

35. Opelt CV, Becker D, Lepienski CM, Coelho LAF. Reinforcement and Toughening mechanisms in polymer nanocomposites: carbon nanotubes and aluminum oxide. Compos, Part B Eng. 2015;75:119-26. http://dx.doi.org/10.1016/j.compositesb.2015.01.019.

36. Bello RH, Coelho LAF, Becker D. Role of chemical funcionalization of carbon nanoparticles in epoxy matrices. J Compos Mater. 2018;52(4):449-64. http://dx.doi.org/10.1177/0021998317709082.

37. Sene TS, Ramos A, Becker D, Coelho LAF. Electrical conductivity behavior of epoxy matrix nanocomposites with simultaneous dispersion of carbon nanotubes and clays. Polym Compos. 2016;37(5):1603-11. http://dx.doi.org/10.1002/pc.23332.

38. Giacometti JA, Carvalho AJF. Condução elétrica. In: Canevarolo SV Jr, editor. Técnicas de caracterização de polímeros. São Paulo: Artliber; 2004. 448 p.

39. Qiao R, Deng H, Putz KW, Brinson LC. Effect of particle agglomeration and interphase on the glass transition temperature of polymer nanocomposites. J Polym Sci, B, Polym Phys. 2011;49(10):740-8. http://dx.doi.org/10.1002/polb.22236.

40. Tsagaropoulos G, Eisenberg A. Dynamic mechanical study of the factors affecting the two glass transition behavior of filled polymers. similarities and differences with random ionomers. Macromolecules. 1995;28(18):6067-77. http://dx.doi.org/10.1021/ma00122a011.

41. Putz KW, Palmeri MJ, Cohn RB, Andrews R, Brinson LC. Effect of cross-link density on interphase creation in polymer nanocomposites. Macromolecules. 2008;41(18):6752-6. http://dx.doi.org/10.1021/ma800830p.

42. Tanaka T, Kozako M, Fuse N, Ohki Y. Proposal of a multi-core model for polymer nanocomposites dielectrics. IEEE Trans Dielectr Electr Insul. 2005;12(4):669-81. http://dx.doi.org/10.1109/TDEI.2005.1511092.

43. Long D, Lequeux F. Heterogeneous dynamics at the glass transition in van der Waals liquids, in the bulk and in thin films. Eur Phys J E. 2001;4(3):371-87. http://dx.doi.org/10.1007/s101890170120.

44. Berriot J, Montes H, Lequeux F, Long D, Sotta P. Evidence for the shift of the glass transition near the particles in silica-filled elastomers. Macromolecules. 2002;35(26):9756-62. http://dx.doi.org/10.1021/ma0212700.

45. Pereira BS. Avaliação da morfologia e propriedades mecânicas de compósitos de estrutura sanduíche a base de epóxi e cortiça [dissertation]. Teresina: Instituto Federal de Educação, Ciência e Tecnologia do Piauí; 2018.

46. Opelt CV, Coelho LAF. Reinforcement and toughening mechanisms in polymer nanocomposites: reinforcement effectiveness and nanoclay nanocomposites. Mater Chem Phys. 2016;169:179-85. http://dx.doi.org/10.1016/j.matchemphys.2015.11.047.

47. Opelt CV, Souza CSR, Marlet JMF, Candido GM, Rezende MC. Compression failure modes of carbon fiber fabric scraps/epoxy laminates. Adv Mat Res. 2016;1135:52-61. http://dx.doi.org/10.4028/www.scientific.net/AMR.1135.52.

48. Schuster MB, Coelho LAF. Toughness and roughness in hybrid nanocomposites of an epoxy matrix. Polym Eng Sci. 2019;59(6):1258-69. http://dx.doi.org/10.1002/pen.25109.

49. Martinez-Garcia JC, Serraïma-Ferrer A, Lopeandía-Fernández A, Lattuada M, Sapkota J, Rodríguez-Viejo J. A Generalized approach for evaluating the mechanical properties of polymer nanocomposites reinforced with spherical fillers. Nanomaterials. 2021;11(4):830. http://dx.doi.org/10.3390/nano11040830.

50. Zare Y, Rhee KY. Evaluation of mechanical properties in nanocomposites containing carbon nanotubes below and above percolation threshold. JOM. 2017;69(12):2762-7. http://dx.doi.org/10.1007/s11837-017-2294-x.

51. Molinari N, Sutton AP, Mostofi AA. Mechanisms of reinforcement in polymer nanocomposites. Phys Chem Chem Phys. 2018;20(35):23085-94. http://dx.doi.org/10.1039/C8CP03281E.

52. Sumfleth J, Prehn K, Wichmann MHG, Wedekind S, Schulte K. A comparative study of the electrical and mechanical properties of epoxy nanocomposites reinforced by CVD- and arc-grown multi-wall carbon nanotubes. Compos Sci Technol. 2010;70(1):173-80. http://dx.doi.org/10.1016/j.compscitech.2009.10.007.

53. Alexopoulos ND, Paragkamian Z, Poulin P, Kourkoulis SK. Fracture related mechanical properties of low and high graphene reinforcement of epoxy nanocomposites. Compos Sci Technol. 2017;150:194-204. http://dx.doi.org/10.1016/j.compscitech.2017.07.030.

54. Zhao X, Li Y, Chen W, Li S, Zhao Y, Du S. Improved fracture toughness of epoxy resin reinforced with polyamide 6/graphene oxide nanocomposites prepared via in situ polymerization. Compos Sci Technol. 2019;171:180-9. http://dx.doi.org/10.1016/j.compscitech.2018.12.023.

55. Chou T-W, Gao L, Thostenson ET, Zhang Z, Byun J-H. An assessment of the science and technology of carbon nanotube-based fibers and composites. Compos Sci Technol. 2010;70(1):1-19. http://dx.doi.org/10.1016/j.compscitech.2009.10.004.

56. Jiménez-Suárez A, Campo M, Gaztelumendi I, Markaide N, Sánchez M, Ureña A. The influence of mechanical dispersion of MWCNT in epoxy matrix by calendering method: batch method versus time controlled. Compos, Part B Eng. 2013;48:88-94. http://dx.doi.org/10.1016/j.compositesb.2012.12.011.

57. Pekturk HY, Elitas M, Goktas M, Demir B, Birhanu S. Evaluation of the effect of MWCNT amount and dispersion on bending fatigue properties of non-crimp CFRP composites. Eng Sci Technol Int J Sci Technol. 2022;34:101081. http://dx.doi.org/10.1016/j.jestch.2021.101081.